Electronic phase conversion by photoinjection of excitations

Kazuki Koshino*
Department of Physics, Tohoku University, Aoba-ku, Sendai 980-8578, Japan
and Institute of Physics, University of Tokyo, 3-8-1 Komaba, Tokyo 153-8902, Japan

Tetsuo Ogawa†
Department of Physics, Tohoku University, Aoba-ku, Sendai 980-8578, Japan
and ''Structure and Transformation,'' PRESTO, Japan Science and Technology Corporation (JST), Japan
(Received 2 June 1999; revised manuscript received 4 October 1999)

We theoretically discuss the photoinduced electronic phase conversion mediated by the electronic interactions, using a phenomenological model of bistable electrons and the modified Hubbard model. We focus on the dynamics after photoexcitation into one of the (meta)stable states of the multistable electronic systems. When small amount of excitations are injected, they merely induce small oscillations in the electronic states. On the other hand, when larger amounts of excitations than a threshold value are injected, they successfully induce large oscillations in the electronic states, which we can regard as the phase conversions. Conditions for induction of the phase conversion are clarified; such induction by photoinjection of a small amount of excitations is possible when the mixing of the two electronic states is large in the initial (meta)stable state.

I. INTRODUCTION

Photoexcitations in a crystal usually result in microscopic changes in the states of electrons and lattices. In recent years, however, many exotic materials are successively found[1–7] where a macroscopic phase transition is induced by photoinjection of excitations into the crystal. Such phenomena are called the photoinduced phase transitions, and have been attracting much attention from both the chemical and physical points of view.

Such phenomena have been found in quite various kinds of materials with multistability, e.g., charge-transfer (CT) complexes,[2,3] π-conjugated polymers,[4,5] and so on. The multistability of the system as well as the interaction among the constituents is brought about by different physical mechanisms in each material, and the phenomena have not been understood from a unified viewpoint. One of such phenomena which are most clearly understood is the photoinduced structural phase transition in quasi-one-dimensional electron-lattice systems such as π-conjugated polymers[8] and metal-halogen chains.[9] In these materials, bistability (two dimerization patterns in the ground state) is brought about by the Peierls mechanism through the electron-lattice interaction and the one dimensionality. Furthermore, instability of a photoinjected electron-hole pair against the adiabatic lattice relaxation to soliton pairs can be understood by the model of noninteracting electrons, where only the electron-lattice interaction is taken into account. Thus we can regard that the photoinduced cooperative structural change in these systems take place mainly due to the electron-lattice interaction, and the electronic correlation plays an auxiliary role.

In some photoinduced phenomena, however, the multistability of the system and the driving force of the cooperative dynamics are attributed to the electronic interactions. The photoinduced cooperative charge transfer in the organic CT complexes belongs to this type. In this system, multistability in the electronic configuration (neutral and ionic phases) originates in the Coulomb interaction among the electrons, i.e., the competition between the loss of ionization energy and the gain in the Madelung energy. The dimerization of the lattice also occurs in the ionic phase through the spin-Peierls mechanism,[10] which is, however, a secondary process following the charge transfer. The mechanism of the photoinduced cooperative phenomena in such systems where the electronic interaction plays a crucial role has not clarified yet from theoretical viewpoints, in contrast to transparency in the electron-lattice systems.

The aim of this study is to investigate the photoinduced phase transition mediated only by the electronic correlation and to reveal the basic mechanisms and conditions for the phenomena. In Sec. II, the photoinduced electronic phase transition is considered from a general viewpoint with a phenomenological model composed of two-level electrons with level crossings due to the interaction among the electrons. The bistability of the electronic system and the mechanism of self-proliferation of the excited states are discussed there. We discuss the conditions for induction of the phase conversion, and show that induction of the phase conversion is possible by injection of small amount of excitations. In Sec. III, we demonstrate how the mechanism investigated in Sec. II is realized in real electronic systems, starting from the modified Hubbard model which describes the electrons in a mixed-stack CT complex from microscopic viewpoint, and applying the unrestricted Hartree-Fock (UHF) approximation. The theoretical results are concluded in Sec. IV with some remarks on the neglected effects in our treatment.

II. PHENOMENOLOGICAL CONSIDERATION ON PHOTOINDUCED PHASE CONVERSION

Our main concern in this paper is the photoinduced dynamics in electronic systems where multistability is brought about by strong interaction among electrons. For example, in the mixed-stack CT complexes, there are two (meta)stable

electronic phases around the critical temperature of the thermal phase transition; one is the neutral (N) phase $[\cdots D^0A^0D^0A^0D^0A^0\cdots]$, where the degree of CT from the donor molecules (D) to the acceptor molecules (A) is almost zero, and the other one is the ionic (I) phase $[\cdots D^+A^-D^+A^-D^+A^-\cdots]$, where the degree of CT is almost unity. In N phase, an ionic DA pair (D^+A^-) is energetically higher than a neutral one (D^0A^0), and is called a CT exciton. On the other hand, in I phase, a neutral one is higher in energy than an ionic one, and is called, again, a CT exciton. Thus the energy difference between neutral and ionic DA pairs is dependent on the degree of CT in the crystal, and inversion in their energies occurs at some degree of CT. Both the $N\rightarrow I$ and $I\rightarrow N$ transitions can be induced by photoinjection of excitations in each phase. In this section, we phenomenologically consider such a situation with a simple bistable electronic system from a general viewpoint.

A. Bistable model

In order to investigate a general situation of photoexcitation in multistable electronic systems, we here employ a phenomenological system composed of two-level electrons, each of which is a linear combination of A state $|A\rangle$ and B state $|B\rangle$, which correspond to the neutral and ionic states of a DA pair in the above example. The Hamiltonian for a two-level electron takes the following form, which is dependent on time τ through the degree $n(\tau)$ of B state (B degree, hereafter) of the total electrons in the system:

$$\mathcal{H}(\tau)=\begin{bmatrix} n(\tau)-m & t \\ t & m-n(\tau) \end{bmatrix}+f(n), \tag{1}$$

where t is the coupling between A and B states, and m is the B degree at which inversion in the energies of the two electronic states takes place. The B degree $n(\tau)$ is the order parameter in this system satisfying $0\leqslant n(\tau)\leqslant 1$. The last c-number term $f(n)=(n-m)(n-1+m)$, which does not affect the dynamics, is added to the Hamiltonian to assure the conservation of energy. This term is naturally introduced when we start from a microscopic Hamiltonian, as shown in Sec. III. It should be noted that the interaction among the electrons is incorporated in the Hamiltonian in the mean-field-like form as the n dependence of the diagonal elements. Equivalence of all two-level electrons due to the mean-field form of the interaction allows us to represent the state of the whole electrons in the system by a single density matrix as

$$\rho(\tau)=\begin{bmatrix} 1-n(\tau) & x(\tau)+\mathrm{i}y(\tau) \\ x(\tau)-\mathrm{i}y(\tau) & n(\tau) \end{bmatrix}. \tag{2}$$

If we neglect the dissipative effects and treat this system as a closed one, the temporal evolution of the density matrix is governed by the following equation:

$$i\frac{d\rho}{d\tau}=[\mathcal{H}(\tau),\rho], \tag{3}$$

which is equivalent to the following Bloch equations:

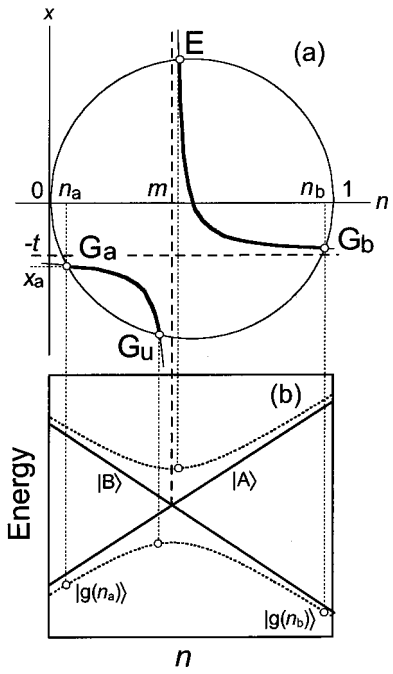

FIG. 1. (a) Stationary density matrices of the Bloch equations. Continuum of the stationary density matrices is drawn by the bold curves. The four points (G_a, G_b, E, and G_u) represent the pure stationary density matrices. (b) Corresponding energies to those four states. The n dependence of the energies of $|A\rangle$ and $|B\rangle$ [$|e(n)\rangle$ and $|g(n)\rangle$] is also shown by the solid (broken) lines.

$$\frac{dn}{d\tau}=2ty, \tag{4}$$

$$\frac{dx}{d\tau}=2(n-m)y, \tag{5}$$

$$\frac{dy}{d\tau}=-2t\left(n-\frac{1}{2}\right)-2(n-m)x. \tag{6}$$

B. Stable and metastable states

First, we investigate the (meta)stable electronic states of this system. As the criteria for the (meta)stable states, we employ the following two conditions; (i) the state is stationary and stable against small fluctuation in n, and (ii) all electrons are in the lower energy eigenstates. The latter condition is necessary because $|e(n)\rangle$ represents an excited electronic state and is unstable against radiative or nonradiative decay to $|g(n)\rangle$, though not explicitly expressed in the equations of motion.

From the Bloch equations, it is easily confirmed that the stationary density matrices are represented by the continuum of the points satisfying $y=0$ and $x=-t(n-1/2)/(n-m)$ inside the circle $(n-1/2)^2+x^2=(1/2)^2$, as shown in Fig. 1(a). These stationary density matrices can be written in the form

$$\rho_n^{\mathrm{st}}=\beta|e(n)\rangle\langle e(n)|+(1-\beta)|g(n)\rangle\langle g(n)|, \tag{7}$$

where $|e(n)\rangle$ ($|g(n)\rangle$) is the higher (lower) energy eigenfunction of the Hamiltonian (1) at fixed n, and β is a real constant satisfying $0\leqslant\beta\leqslant 1$.

The pure ($\beta=0$ or 1) stationary density matrices are represented in Fig. 1(a) by the intersections of the circle and the hyperbola, and their energies are shown in Fig. 1(b). Among these four points (G_a, G_b, E, and G_u) in Fig. 1(a), E represents a stable stationary state with every electrons in the higher energy eigenstate, and G_u corresponds to an unstable stationary state with every electrons in the lower energy eigenstate, so these two states cannot be regarded as the (meta)stable states. However, G_a and G_b represent (meta)-stable stationary states with every electrons in the lower energy eigenstate. We hereafter call these states A- and B-dominant phases, respectively, the density matrix of which are given by $\rho_A=|g(n_a)\rangle\langle g(n_a)|$ and $\rho_B=|g(n_b)\rangle\langle g(n_b)|$, where n_a and n_b is defined in Fig. 1(a). When $m-\frac{1}{2}$ is positive (negative), the A-dominant phase is the stable (metastable) state.

In fact, the system has these two states only when t and $|m-1/2|$ are small enough to satisfy

$$t\leqslant\left[\left(\frac{1}{2}\right)^{2/3}-\left|m-\frac{1}{2}\right|^{2/3}\right]^{3/2}. \tag{8}$$

If this condition is not satisfied, there are only two intersections in Fig. 1(a), i.e., G_a (G_b) and E, and the system has only the $A(B)$-dominant phase as a stable electronic state.

C. Temporal evolution after photoexcitation

Now we start investigating temporal evolution of the system after photoinjection of excitations into one of the (meta-)stable states, e.g., the A-dominant phase. We consider the simplest situation that some amount of electrons in the A-dominant phase are simultaneously photoexcited from the ground state $|g(n_a)\rangle$ to the excited state $|e(n_a)\rangle$ at $\tau=0$. The density matrix just after photoexcitation is then given by

$$\rho(0)=\phi|e(n_a)\rangle\langle e(n_a)|+(1-\phi)|g(n_a)\rangle\langle g(n_a)|, \tag{9}$$

where ϕ ($0\leqslant\phi\leqslant1$) represents the fraction of the injected excitations. This density matrix is no longer stationary as long as $\phi\neq0$, and starts evolution according to the Bloch equations.

We can easily find two constants of motion, namely, the purity $\mathcal{P}$ of the density matrix and the energy $\langle\mathcal{H}\rangle$, which are given by

$$\mathcal{P}=1/4-\det\rho=(1/2-\phi)^2, \tag{10}$$

$$\langle\mathcal{H}\rangle=2tx-(n-m)^2=2tx_0-(n_0-m)^2. \tag{11}$$

Here n_0 and x_0 are determined by the density matrix (9), which are given, using n_a and x_a defined in Fig. 1(a), by

$$n_0\equiv n(0)=(1-\phi)n_a+\phi(1-n_a), \tag{12}$$

$$x_0\equiv x(0)=(1-\phi)x_a+\phi(-x_a). \tag{13}$$

The temporal evolution of n is governed by the following classical equation of motion:

$$\frac{d^2n}{d\tau^2}=-\frac{d}{dn}V(n), \tag{14}$$

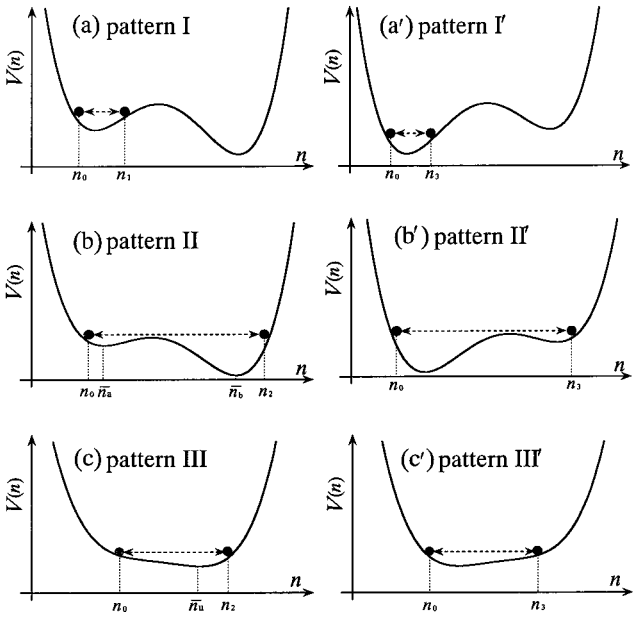

FIG. 2. The potential $V(n)$ and the initial position n_0 for (a) small ϕ ($\phi<\phi_{I-II}$), (b) intermediate ϕ ($\phi_{I-II}<\phi<\phi_{II-III}$), and (c) large ϕ ($\phi_{II-III}<\phi$), starting from the metastable phase. Three possible patterns of the dynamics of $n(\tau)$ starting from the stable phase are drawn in (a′), (b′), and (c′).

with the initial conditions $n(0)=n_0$ and $(dn/d\tau)(0)=0$, where the ''potential'' $V(n)$ is given by

$$V(n)=\frac{(n-m)^4}{2}+2t^2\left(n-\frac{1}{2}\right)^2-[(n_0-m)^2-2tx_0](n-m)^2. \tag{15}$$

In the following, we restrict ourselves to the case where the system is bistable, i.e., the condition (8) is satisfied.

1. Photoexcitation into the metastable phase

First we investigate the dynamics after photoexcitation into the metastable phase. To this end, we consider the case of $m<\frac{1}{2}$, where A-dominant phase is the metastable phase. In Figs. 2(a)–2(c), the potential $V(n)$ and the initial position n_0 are drawn for small, intermediate, and large values of ϕ, respectively.

When no excitations are injected, i.e., $\phi=0$, $V(n)$ takes the form of a double-well potential and $n(\tau)$ rests at the metastable minimum of the potential, which implies that the A-dominant phase is stationary in agreement with our preceding discussion.

For small ϕ ($\phi<\phi_{I-II}$), $n(\tau)$ oscillates *locally* around the metastable minimum of the potential in Fig. 2(a) with the period $2\tau_1$ of an order unity, which we hereafter call pattern I. At half integer times of the period, the density matrix of the system takes the following form:

$$\rho(\tau_1)=\phi|e(n_a')\rangle\langle e(n_a')|+(1-\phi)|g(n_a')\rangle\langle g(n_a')|, \tag{16}$$

where n_a' is determined, through n_1 defined in Fig. 2(a), by the relation $n_1=(1-\phi)n_a'+\phi(1-n_a')$. Because n_a' is close to n_a in this case, the density matrix (16) represents a state

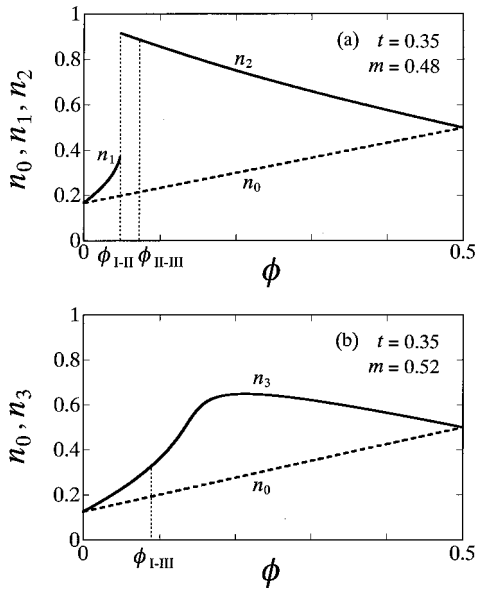

FIG. 3. The maximum B degree (n_1, n_2, and n_3 in Fig. 2) as a function of the fraction ϕ of injected excitation, (a) when the initial A-dominant phase is metastable ($m=0.48$ and $t=0.35$), and (b) when the initial B-dominant phase is stable ($m=0.52$ and $t=0.35$). n_0 is also plotted by the broken line.

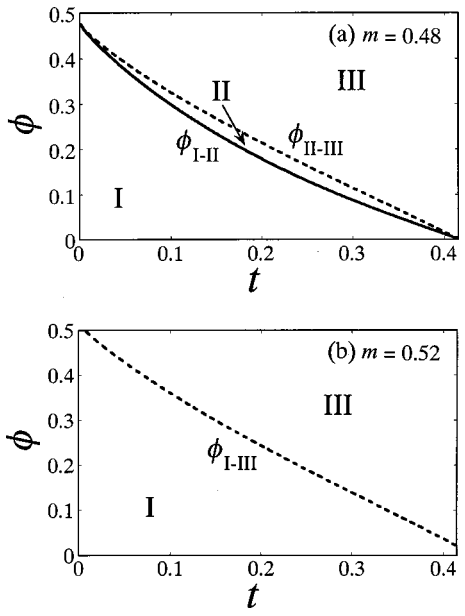

FIG. 4. Relation between the fraction ϕ of injected excitations and resulting patterns of dynamics (a) from the initial metastable phase ($m=0.48$) and (b) from the stable phase ($m=0.52$). The dynamics changes discontinuously at the solid ''phase'' boundary [$\phi_{\text{I-II}}$ in (a)] between the local and global oscillation, while it changes continuously around the dotted curves [$\phi_{\text{II-III}}$ in (a) and $\phi_{\text{I-III}}$ in (b)], i.e., crossover behavior is seen.

where the B degree is slightly increased (decreased) in the ground (excited) state compared to the initial state (9).

On the other hand, $n(\tau)$ oscillates *globally* in the double-well potential in Fig. 2(b) for intermediate ϕ ($\phi_{\text{I-II}}<\phi<\phi_{\text{II-III}}$), or the oscillation occurs in a single-well potential in Fig. 2(c) for large ϕ ($\phi_{\text{II-III}}<\phi$), which we hereafter call patterns II and III, respectively. The period $2\tau_2$ of the oscillation is of an order unity except the neighbor to the boundary to pattern I, where τ_2 becomes a large value. The state at half integer times of the period takes the following form:

$$\rho(\tau_2)=\phi|e(n_{\text{b}}')\rangle\langle e(n_{\text{b}}')|+(1-\phi)|g(n_{\text{b}}')\rangle\langle g(n_{\text{b}}')|, \tag{17}$$

where n_{b}' is determined, through n_2 defined in Fig. 2(b) or 2(c), by the relation $n_2=(1-\phi)n_{\text{b}}'+\phi(1-n_{\text{b}}')$. In contrast to pattern I, n_{b}' is close to n_{b} in this case ($n_{\text{b}}'=n_{\text{b}}$ holds when $m=\frac{1}{2}$), and the density matrix $\rho(\tau_2)$ represents the inverted situation from the initial one $\rho(0)$, i.e., excitations are injected in the B-dominant phase. We can therefore regard that injection of excitations into the A-dominant phase successfully induces the phase conversion to B-dominant phase in this case. Due to our treatment of this system as a closed one, $\rho(\tau_2)$ returns to the initial state (9) at integer times of the period, and this oscillation between $\rho(0)$ and $\rho(\tau_2)$ continues eternally.

The maximum B-degree (n_1 or n_2 in Figs. 2) is plotted in Fig. 3(a) as a function of ϕ. The figure demonstrates the drastic change of the dynamics at $\phi=\phi_{\text{I-II}}$, which should be regarded as the threshold fraction of injected excitations for phase conversion; injection of smaller amount of excitations than the threshold value only results in small oscillation in the electronic states, while injection of larger amount induces large oscillation, which can be regarded as the phase conversions. The key mechanism to yield such discrimination is that the self-increase of n effectively occurs in the region of n satisfying $|n-m|\lesssim t$, i.e., the neighborhood of the level-crossing point. In this region, increase in n adiabatically induces the increase (decrease) of the B degree in the ground-(excited-)state electrons, which totally results in the increase of n if $\phi<\frac{1}{2}$. Qualitatively speaking, the phase conversion takes place when the initial trigger for the oscillation (photoinjection of excitations) is intensive enough to drive $n(\tau)$ to reach the region.

The relation between ϕ and three resulting patterns are summarized in Fig. 4(a), which indicates the possibility of induction of the phase conversions by even small ϕ for large t, i.e., where the B degree n is large in the initial A-dominant phase due to quantum mixing. In this case, the initial state is close to the self-increase region of n even without photoinjection, and small injection of excitations is enough to induce the phase conversion. If the interaction among the constituents is short ranged or the system is a low-dimensional one, the phase conversion may be induced by further smaller injection than is predicted in this study where a long-ranged interaction is adopted.

2. Photoexcitation into the stable phase

Next, we discuss the dynamics after photoexcitation into the stable phase. We treat the case of $m>\frac{1}{2}$, where A-dominant phase corresponds to the stable one. For small ϕ, $V(n)$ has two minima and $n(\tau)$ oscillates locally around the stable minimum [Fig. 2(a′), pattern I′]. As we increase ϕ, there are two possibilities; the oscillation becomes a global one in a double-well potential [Fig. 2(b′), pattern II′], or $V(n)$ becomes a single-well potential [Fig. 2(c′), pattern III′]. Only in the restricted situation where the A- and

B-dominant phases are almost degenerate, i.e., m is very close to $\frac{1}{2}$, the dynamics changes as patterns $\mathrm{I}' \rightarrow \mathrm{II}' \rightarrow \mathrm{III}'$ by increasing ϕ. Except for such special cases, pattern II' never appears; the dynamics changes from pattern I' to III' directly at $\phi = \phi_{\mathrm{I}'-\mathrm{III}'}$. This is, however, only the change in the form of the potential $V(n)$, and makes no qualitative difference in the motion of $n(\tau)$. Thus the maximum B degree changes cotinuously by increasing ϕ, as shown in Fig. 3(b). In Fig. 4(b), $\phi_{\mathrm{I-III}}$ is plotted as a function of t. As mentioned above, dynamics of $n(\tau)$ changes gradually from patterns I' to III' around the ''phase'' boundary $\phi_{\mathrm{I-III}}$, contrary to the drastic change at $\phi_{\mathrm{I-II}}$ in Fig. 4(a).

3. Degenarate case

In the above discussion, we have observed that the dynamics after photoinjection into the *metastable* phase always changes as patterns $\mathrm{I} \rightarrow \mathrm{II} \rightarrow \mathrm{III}$ by increasing ϕ, with drastic change at the threshold value $\phi_{\mathrm{I-II}}$, while the dynamics after photoinjection into the *stable* phase changes continuously from pattern I' to III' as we increase ϕ, unless the two phases are almost degenerate. When two phases are almost degenerate, however, the abrupt change at the threshold value can be observed from both *A*- and *B*-dominant phases.

The phase boundaries in Fig. 4(a) is analytically given for $m = \frac{1}{2}$ by

$$\phi_{\mathrm{I-II}}(t) = \frac{1-2t}{2(1+2t)}, \tag{18}$$

$$\phi_{\mathrm{II-III}}(t) = \frac{1-\sqrt{1-(1-4t^2)^2}}{2(1-4t^2)}. \tag{19}$$

When t is large, i.e., the mixing of two electronic states is large in the initial state, phase conversion can be induced by small ϕ from *both A*- and *B*-dominant phases.

D. Effect of dissipation

In the dynamics discussed above, oscillation of $n(\tau)$ continues eternally without damping, and therefore patterns II and III cannot be distinguished clearly by the motion of $n(\tau)$. The difference between these two patterns, however, will be clarified by taking account of the effects of relaxation such as dephasing and energy dissipation due to the coupling to phonon modes in the crystal, the photon field, and so on. For example, we consider the effect of dephasing by the following equation:

$$i\frac{d\rho}{d\tau} = [\mathcal{H}(\tau), \rho] - i\Gamma[\langle e(n)|\rho|g(n)\rangle |e(n)\rangle\langle g(n)| + \mathrm{H.\,c.}], \tag{20}$$

where Γ represents the dephasing rate. During the evolution by Eq. (20), the energy $\langle \mathcal{H} \rangle$ defined in Eq. (11) is conserved, while the purity $\mathcal{P}$ defined in Eq. (10) decreases monotonously. Roughly speaking, oscillation of $n(\tau)$ damps as a result of dephasing.

In pattern II, depending on the dephasing rate Γ, n relaxes to $\overline{n_{\mathrm{a}}}$ or $\overline{n_{\mathrm{b}}}$ in Fig. 2(b). For example, if n relaxes to $\overline{n_{\mathrm{b}}}$, the density matrix for the relaxed state is

$$\rho_{\mathrm{b}}(\infty) = \phi' |e(\overline{n_2})\rangle\langle e(\overline{n_2})| + (1-\phi')|g(\overline{n_2})\rangle\langle g(\overline{n_2})|, \tag{21}$$

where ϕ' is a constant satisfying $|\phi' - \frac{1}{2}| < |\phi - \frac{1}{2}|$, i.e., the purity of the system is decreased, and $\overline{n_2}$ is determined by the relation $\overline{n_2} = (1-\phi')\overline{n_{\mathrm{b}}} + \phi'(1-\overline{n_{\mathrm{b}}})$. The excited-state electrons later decay to the ground states radiatively or nonradiatively, and finally the system reaches to *B*-dominant phase. If n relaxes to $\overline{n_{\mathrm{a}}}$, the system returns to *A*-dominant phase. It depends on Γ to which phase the system finally relaxes.

On the other hand, in pattern III, n always relaxes to $\overline{n_{\mathrm{u}}}$ in Fig. 2(c). In this case, after the decay of the excited-state electrons, the system always relaxes to the lower energy phase in the end, i.e., to *B*-dominant phase if $m < \frac{1}{2}$. Thus the dephasing introduces a clear distinction between patterns II and III; relaxation to *A*- or *B*-dominant phases takes quite different paths.

E. Summary

We have investigated the dynamics induced by photoinjection of excitations into a bistable electronic system, using a phenomenological model composed of interacting two-level electrons. First, we have clarified two (meta)stable states of this system, i.e., *A*- and *B*-dominant phases. Then, we have discussed in detail the dynamics after photoinjection of excitations into the *A*-dominant phase.

If the initial *A*-dominant phase is metastable, the dynamics of $n(\tau)$ always changes as patterns $\mathrm{I} \rightarrow \mathrm{II} \rightarrow \mathrm{III}$ by increasing the fraction ϕ of injected excitations [see Figs. 2(a)–2(c)]. The fraction $\phi_{\mathrm{I-II}}$ dividing patterns I and II should be regarded as a threshold fraction for phase conversion. When small amount of excitations are injected ($\phi < \phi_{\mathrm{I-II}}$), it simply results in small oscillation in the electronic states, while, when larger amount of excitations than the threshold value are injected ($\phi_{\mathrm{I-II}} < \phi$), large oscillation in the electronic states is successfully induced, which we can regard as the phase conversions, as shown in Fig. 3(a). On the other hand, when the initial *A*-dominant phase is the stable one, the dynamics of $n(\tau)$ changes from patterns I' to III' as we increase ϕ [see Figs. 2(a) and 2(c)], unless the two phases are almost degenerate. The dynamics changes continuously as shown in Fig. 3(b). Only when the two phases are almost degenerate, thresholdlike behavior in ϕ can be observed, starting from both phases.

The relation between ϕ and resulting patterns of dynamics is summarized in Fig. 4, which indicates that the phase conversion can be induced even by small injection of excitations when t is large, i.e., the mixing of the two electronic states is large in the initial *A*-dominant phase.

III. PHOTOINDUCED COOPERATIVE CHARGE TRANSFER IN MIXED-STACK CHARGE-TRANSFER COMPLEXES

In the previous section, we have investigated the dynamics triggered by photoinjection of excitations into a bistable electronic system, and have shown that the electronic phase conversion is induced when more excitations than the threshold value is injected. The model employed there is, however,

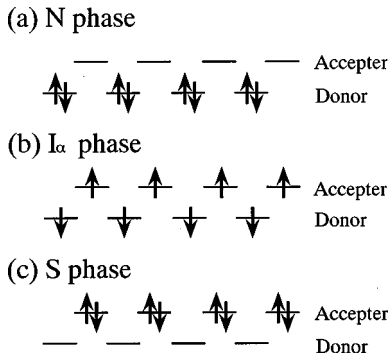

FIG. 5. The electronic configurations in (a) N phase, (b) I_α phase, and (c) S phase, for $T=0$. The configuration in I_β phase is obtained by changing α (up) and β (down) spin electrons.

introduced *phenomenologically* to describe a general situation of electronic bistability, and the correspondence of this model to real systems is still unclear. In this section, starting from the modified Hubbard Hamiltonian, which describes the electrons in a mixed-stack CT complex from a *microscopic* viewpoint, we discuss how the mechanism presented in the previous section is realized in this electronic system.

A. Modified Hubbard model

Our discussion in this section is based on the following one-dimensional tight-binding Hamiltonian,

$$\mathcal{H}=-T\sum_{j,\sigma}(c_{j\sigma}^{\dagger}c_{j+1,\sigma}+c_{j+1,\sigma}^{\dagger}c_{j\sigma})+\frac{\Delta}{2}\sum_{j,\sigma}(-1)^{j}n_{j\sigma}+U\sum_{j}n_{j\alpha}n_{j\beta}-\frac{NM}{2}n_{\mathrm{A}}^{2}, \tag{22}$$

where odd (even) sites represent the HOMO (LUMO) of a donor (accepter) molecule, $c_{j\sigma}$, $c_{j\sigma}^{\dagger}$, and $n_{j\sigma}$ are the annihilation, creation, and number operator for an electron with spin σ ($=\alpha$ or β) at the jth site. The total number of the electrons, which is equal to the number of the sites, is denoted by N, and $n_{\mathrm{A}}=(2/N)\Sigma_{j:\mathrm{even},\sigma}n_{j\sigma}$ measures the ionicity of the complex. The meaning of the parameters are the following; T is the nearest-neighbor CT integral, Δ is the energy difference between the donor and accepter orbitals, U is the on-site Coulomb repulsion, and M is the Madelung stabilization energy.

In order to grasp the (meta)stable electronic states and the CT excitation energies from each state, we first consider the case of $T=0$ where classical treatment of electrons is allowed. We here define the degree η_σ of CT for σ-spin electrons by

$$\eta_\sigma=\frac{2}{N}\sum_{j:\mathrm{even}}\langle n_{j\sigma}\rangle. \tag{23}$$

There are four candidates of (meta)stable states; a neutral phase ($\eta_\alpha=\eta_\beta=0$), two ionic phases ($\eta_\alpha=1,\eta_\beta=0$ and $\eta_\alpha=0,\eta_\beta=1$), and a superionic phase ($\eta_\alpha=\eta_\beta=1$), which we hereafter call N, I_α, I_β, and S phase, respectively. The electronic configurations for these phases are shown in Fig. 5, and their energies, CT excitation energies and conditions for existence of each phase are summarized in Table I. We can easily see that this electronic system has multistability under an appropriate choice of the parameters. In this study, we choose the parameters to satisfy

$$0<\frac{\Delta-U}{2}<M<\frac{\Delta+U}{4}, \tag{24}$$

in which case the system has three (meta)stable phases (N, I_α, and I_β) for $T=0$, considering the experimental fact that the S phase has not been observed in the CT complexes. To treat the general case of nonzero T, we introduce the Bloch orbitals defined by

$$d_{k\sigma}=\sqrt{\frac{2}{N}}\sum_{j:\mathrm{even}}e^{\mathrm{i}k(j-1)}c_{j-1,\sigma}, \tag{25}$$

$$a_{k\sigma}=\sqrt{\frac{2}{N}}\sum_{j:\mathrm{even}}e^{\mathrm{i}kj}c_{j\sigma}, \tag{26}$$

with $k=0,\pm 2\pi/N,\ldots,\pm\pi/2$. In terms of these operators, the Hamiltonian (22) is rewritten as

$$\mathcal{H}=-\sum_{k,\sigma}T_k(a_{k\sigma}^{\dagger}d_{k\sigma}+d_{k\sigma}^{\dagger}a_{k\sigma})(a_{k\sigma}^{\dagger}a_{k\sigma}-d_{k\sigma}^{\dagger}d_{k\sigma}) \tag{27}$$

TABLE I. Candidates of the (meta)stable states for $T=0$. The characteristics of the I_β phase is obtained from that of the I_α phase by changing the spin indices α and β.

Phase	N	I_α	S
Order parameters	$\eta_\alpha=\eta_\beta=0$	$\eta_\alpha=1,\eta_\beta=0$	$\eta_\alpha=\eta_\beta=1$
Condition for existence	$E_{\alpha(\beta)}(0,0)=\frac{\Delta-U}{2}>0$	$E_\alpha(1,0)=\frac{\Delta-U}{2}-M<0$ $E_\beta(1,0)=\frac{\Delta+U}{2}-M>0$	$E_{\alpha(\beta)}(1,1)=\frac{\Delta+U}{2}-2M<0$
Energy	$-N\frac{\Delta-U}{2}$	$-\frac{NM}{2}$	$N\left(\frac{\Delta+U}{2}-2M\right)$
Excitation energy	$\epsilon_{\mathrm{CT}}^{\mathrm{N}}=\Delta-U$	$\epsilon_{\mathrm{CT}}^{\mathrm{I}}=-\Delta+U+2M$ $\epsilon_{\mathrm{CT}}^{\mathrm{I}'}=\Delta+U-2M$	$\epsilon_{\mathrm{CT}}^{\mathrm{S}}=-\Delta-U+4M$

$$+\frac{2U}{N}\sum_{k,k',q}(a^{\dagger}_{k+q,\alpha}a^{\dagger}_{k'-q,\beta}a_{k'\beta}a_{k\alpha}$$

$$+d^{\dagger}_{k+q,\alpha}d^{\dagger}_{k'-q,\beta}d_{k'\beta}d_{k\alpha})-\frac{2M}{N}\left(\sum_{k,\sigma}a^{\dagger}_{k\sigma}a_{k\sigma}\right)^2, \quad (28)$$

where $T_k=2T\cos k$. Applying the UHF approximation, we treat the four-operator terms as the energy shift of one-electronic states, each of which is composed by the linear combination of $d^{\dagger}_{k\sigma}$ and $a^{\dagger}_{k\sigma}$.[11,12] Then we get the following Hartree-Fock Hamiltonian:

$$\mathcal{H}^{\mathrm{HF}}=\sum_{k\sigma}[E_{\sigma}(\eta_{\alpha},\eta_{\beta})(a^{\dagger}_{k\sigma}a_{k\sigma}-d^{\dagger}_{k\sigma}d_{k\sigma})$$

$$-T_k(a^{\dagger}_{k\sigma}d_{k\sigma}+d^{\dagger}_{k\sigma}a_{k\sigma})]+f(\eta_{\alpha},\eta_{\beta}), \quad (29)$$

where $E_{\sigma}(\eta_{\alpha},\eta_{\beta})$ is the energy of the one-electronic state given by

$$E_{\sigma}(\eta_{\alpha},\eta_{\beta})\equiv\frac{\Delta-U}{2}-M(\eta_{\sigma}+\eta_{\bar{\sigma}})+U\eta_{\bar{\sigma}}, \quad (30)$$

where $\bar{\sigma}$ is the opposite spin of σ. The last term in Eq. (29) is the *c*-number contribution given by $f(\eta_{\alpha},\eta_{\beta})=-NU(\eta_{\alpha}-1)(\eta_{\beta}-1)/2+NM(\eta_{\alpha}+\eta_{\beta}-1)^2/2$. This Hamiltonian can be recast into the following matrix form:

$$\mathcal{H}^{\mathrm{HF}}=\sum_{k\sigma}\mathcal{H}_{k\sigma}+f(\eta_{\alpha},\eta_{\beta}), \quad (31)$$

where

$$\mathcal{H}_{k\sigma}=\begin{bmatrix}E_{\sigma}(\eta_{\alpha},\eta_{\beta}) & -T_k\\ -T_k & -E_{\sigma}(\eta_{\alpha},\eta_{\beta})\end{bmatrix} \quad (32)$$

is an operator which operates on the density matrix $\rho_{k\sigma}$;

$$\rho_{k\sigma}=\begin{bmatrix}\langle a^{\dagger}_{k\sigma}a_{k\sigma}\rangle & \langle d^{\dagger}_{k\sigma}a_{k\sigma}\rangle\\ \langle a^{\dagger}_{k\sigma}d_{k\sigma}\rangle & \langle d^{\dagger}_{k\sigma}d_{k\sigma}\rangle\end{bmatrix}=\begin{bmatrix}\eta_{k\sigma} & x_{k\sigma}+iy_{k\sigma}\\ x_{k\sigma}-iy_{k\sigma} & 1-\eta_{k\sigma}\end{bmatrix}. \quad (33)$$

It should be noted that the degree η_{σ} of CT is determined by the diagonal elements of the density matrix as $\eta_{\sigma}=(2/N)\Sigma_k\eta_{k\sigma}$.

Under our choice of the parameters, the sign of $E_{\sigma}(\eta_{\alpha},\eta_{\beta})$ changes in the region of $0\leqslant\eta_{\alpha},\eta_{\beta}\leqslant 1$ as shown in Fig. 6, i.e., inversion of energy between the one-electronic states corresponding to $a^{\dagger}_{k\sigma}$ and $d^{\dagger}_{k\sigma}$ takes place as the degree η_{σ} of CT changes. The similarity to the bistable model discussed in Sec. II is now obvious; in both systems, inversion of the ground and excited states is brought about by the whole electronic states in the system. An important difference lies in the point that the level-crossing occurs two dimensionally with two order parameters η_{α} and η_{β}, while it occurs one dimensionally with a single order parameter *n* in the phenomenological bistable model.

B. Stable and metastable states

The candidates of the (meta)stable states is summarized in Table I for the simplest case of $T=0$. In this subsection, we identify the (meta)stable states of this electronic system in the presence of nonzero *T*. The criteria for (meta)stability is the same as the ones employed in Sec. II B; the eigenstates of the Hamiltonian (31) with Eq. (32), with every electron in the lower energy state.

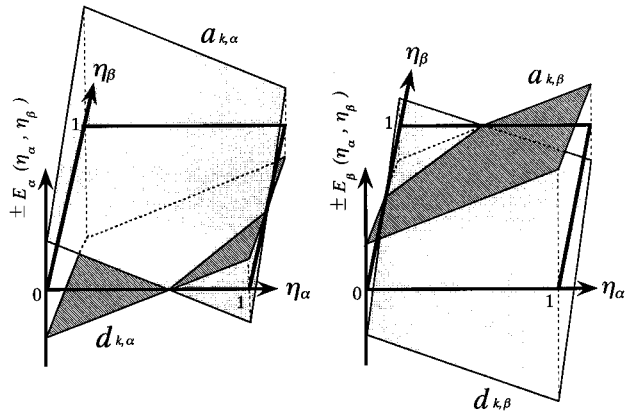

FIG. 6. Conversion between the energies of one-electronic states $a^{\dagger}_{k\sigma}$ and $d^{\dagger}_{k\sigma}$, which are given by $\pm E_{\sigma}(\eta_{\alpha},\eta_{\beta})$ defined in Eq. (30). The parameters are chosen to satisfy the condition (24).

The density matrix of the lower energy state for $\mathcal{H}_{k\sigma}$ is easily given by $\eta_{k\sigma}=\sin^2\theta_{k\sigma}$, $x_{k\sigma}=\sin\theta_{k\sigma}\cos\theta_{k\sigma}$ and $y_{k\sigma}=0$ with $\theta_{k\sigma}$ defined by $\cos 2\theta_{k\sigma}=E_{\sigma}/\sqrt{E^2_{\sigma}+T^2_k}$ and $\sin 2\theta_{k\sigma}=-T_k/\sqrt{E^2_{\sigma}+T^2_k}$. Using these values, the CT degrees $\bar{\eta}_{\alpha}$ and $\bar{\eta}_{\beta}$ for (meta)stable states are determined self-consistently by the following equation:

$$\bar{\eta}_{\sigma}=\frac{2}{N}\sum_k\bar{\eta}_{k\sigma}=\frac{1}{2}-\frac{1}{\pi}\int_0^{\pi/2}dk\frac{E_{\sigma}(\bar{\eta}_{\alpha},\bar{\eta}_{\beta})}{\sqrt{E^2_{\sigma}(\bar{\eta}_{\alpha},\bar{\eta}_{\beta})+T^2_k}}, \quad (34)$$

where the second term can be evaluated as an complete elliptic integral of the first kind.

The solutions of the self-consistent equations are shown in Fig. 7 under the choice (24) of the parameters, where *N*, I_{α}, and I_{β} phases exist for $T=0$. These three phases certainly appear for small *T* as shown in Fig. 7(a). Besides these stable ones, two unstable stationary solutions also exist. However, two stationary solutions (I_{α} and I_{β}) disappears for large *T* as shown in Fig. 7(b), which corresponds to the loss of bistability discussed in Sec. II B. The CT energy *T* is known to be much smaller than other parameters (Δ, *U*, and *M*) in real CT complexes. We hereafter focus on the case of small enough *T* to ensure multistability.

C. Temporal evolution after photoexcitation

Now we start investigating the dynamics triggered by photoinjection of excitations (CT electron-hole pairs) into one of the (meta)stable states. Instead of dealing with the system accurately, we introduce here an approximation for simple treatment of the system. The discrimination among one-electronic states with the same spin is brought about only through the off-diagonal elements T_k of the Hamiltonian (32). We neglect *k* dependence of T_k by putting

$$T_k=\sqrt{2}T, \quad (35)$$

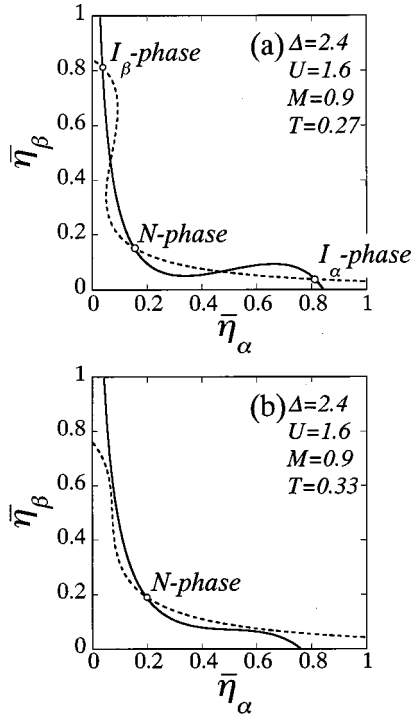

FIG. 7. Stable and metastable electronic states of the system. The solid (broken) line represents the solution of Eq. (34) for spin α (β), and the intersections correspond to the stationary solutions. (a) For small T, the system has three (meta)stable states and two unstable stationary states, but (b) for large T, multistability of the system is lost.

which is equivalent to adding extra hopping to the original Hamiltonian (22), i.e., the first term is replaced by $-\Sigma_{j,m}T_m(c_j^\dagger c_{j+m}+c_{j+m}^\dagger c_j)$ with $T_m=(2\sqrt{2}T/m\pi)\sin(m\pi/4)$. This approximation enables us to treat every one-electronic state with the same spin equivalently. Because the bandwidth introduced by T is much smaller than the band gap ($\sim\epsilon_{\mathrm{CT}}$ in Table I), this approximation does not change the essential features of photoinduced dynamics in this system.

The electronic states of the system is then described by only two density matrices ρ_α and ρ_β, the matrix elements of which we denote by

$$\rho_\sigma=\begin{bmatrix}\eta_\sigma & x_\sigma+\mathrm{i}y_\sigma\\ x_\sigma-\mathrm{i}y_\sigma & 1-\eta_\sigma\end{bmatrix}. \tag{36}$$

The matrix elements $\bar{\eta}_\sigma$, $\bar{x}_\sigma$, and $\bar{y}_\sigma$ for the stable states is determined by the self-consistent Eq. (34) with $T_k^2=2T^2$.

As the initial conditions, we again employ an idealized one that some amount of electrons, ϕ_σ for spin σ, are simultaneously excited at $\tau=0$ from one of the (meta)stable states. The density matrices just after photoexcitation are then given by

$$\rho_\sigma(0)=(1-\phi_\sigma)\begin{bmatrix}\bar{\eta}_\sigma & \bar{x}_\sigma\\ \bar{x}_\sigma & 1-\bar{\eta}_\sigma\end{bmatrix}+\phi_\sigma\begin{bmatrix}1-\bar{\eta}_\sigma & -\bar{x}_\sigma\\ -\bar{x}_\sigma & \bar{\eta}_\sigma\end{bmatrix}. \tag{37}$$

The coherent dynamics from this state is governed by the following Bloch equations:

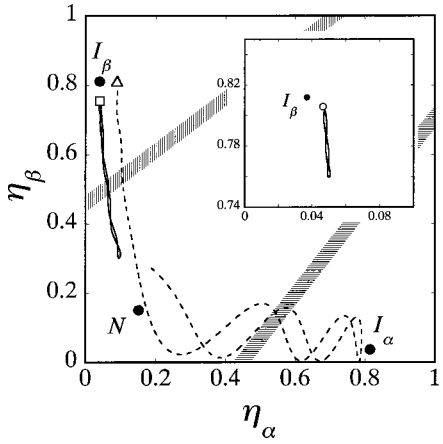

FIG. 8. Temporal trajectories of (η_α,η_β) after photoinjection into the I_β phase; solid [broken] curve for $(\eta_\alpha,\eta_\beta)=(0,0.1)$ [(0.05, 0)]. The square and triangle marks represent the initial condition just after photoexcitation. The vertically (horizontally) shadowed region represents the effective CT region for β- (α-)spin electrons. Inset: motion of (η_α,η_β) after weak excitation, $(\eta_\alpha,\eta_\beta)=(0.01,0.01)$.

$$\frac{d\eta_\sigma}{d\tau}=\sqrt{2}Ty_\sigma, \tag{38}$$

$$\frac{dx_\sigma}{d\tau}=E_\sigma(\eta_\alpha,\eta_\beta)y_\sigma, \tag{39}$$

$$\frac{dy_\sigma}{d\tau}=-E_\sigma(\eta_\alpha,\eta_\beta)x_\sigma-\sqrt{2}T\left(\eta_\sigma-\frac{1}{2}\right). \tag{40}$$

As expected, the purity of the density matrices $[\mathcal{P}_{\alpha(\beta)}=1/4-\det\rho_{\alpha(\beta)}]$ and the energy $[\langle\mathcal{H}\rangle=-\sqrt{2}T(x_\alpha+x_\beta)-M(\eta_\alpha+\eta_\beta)^2/2+U\eta_\alpha\eta_\beta+(\Delta-U)(\eta_\alpha+\eta_\beta-1)/2]$ are conserved during the temporal evolution.

We hereafter fix the parameters to $\Delta=2.4$, $U=1.6$, $M=0.9$, and $T=0.27$ (in units of eV), which are chosen according to several experimental results. Under our choice of parameters, N, I_α, and I_β phases exist as shown in Fig. 7(a). In addition, the thresholdlike behavior in the fraction ϕ_σ of excitation can be observed from both N and I_σ phases under our choice of parameters, which indicates that the three phases are almost degenerate as discussed in Sec. II C. In the following, we discuss the dynamics after photoinjection of excitations into I_σ and N phases, respectively.

1. Temporal evolution from I_β phase

We examine here the dynamics of (η_α,η_β) induced by photoinjection of CT electron-hole pairs into I_β phase, for example. The result from I_α phase can be obtained by exchanging the spin indices α and β in the following discussion. The trajectories of (η_α,η_β) are shown in Fig. 8 under several different excitation conditions. When both ϕ_α and ϕ_β are small, (η_α,η_β) oscillates *locally* around the point representing I_β phase [inset of Fig. 8, for $(\phi_\alpha,\phi_\beta)=(0.01,0.01)$]. However, when ϕ_α and ϕ_β becomes larger, a *global* motion is induced [solid and broken curves in Fig. 8, for $(\phi_\alpha,\phi_\beta)=(0,0.1)$ and $(0.05,0)$, respectively], which can be regarded as phase conversions. The conditions on

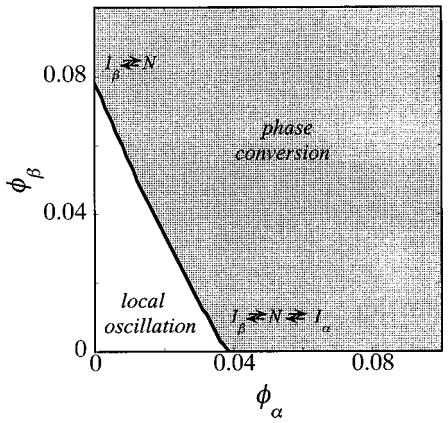

FIG. 9. Relation between the excited fraction $(\phi_\alpha, \phi_\beta)$ and its resultant dynamics, starting from the I_β phase. The dynamics changes qualitatively at the ''phase'' boundary between the local oscillation around the initial position and the global motion which can be regarded as phase conversions.

$(\phi_\alpha, \phi_\beta)$ for induction of phase conversions is summarized in Fig. 9. At the ''phase'' boundary, qualitative change in the dynamics takes place, i.e., thresholdlike behavior in $(\phi_\alpha, \phi_\beta)$ is observed.

The trajectories of $(\eta_\alpha, \eta_\beta)$ plotted in Fig. 8 indicates distinction between the dynamics induced by α-spin excitation and β-spin excitation. When only β-spin electrons are excited, the phase conversion occurs between I_β and N phases (solid curve in Fig. 8). In this case, η_α is kept almost constant during the dynamics, and CT of β-spin electrons mainly takes place. Thus the dynamics can be approximately described by the bistable model discussed in the previous section. On the other hand, when only α-spin electrons are excited, phase conversions occur, roughly speaking, between I_β and I_α phases via the N phase (broken curve in Fig. 8), i.e., CT of β-spin electrons and α-spin electrons take place alternately.

The dynamics just after photoinjection is independent of the spin of injected excitations; only η_β decreases, i.e., β-spin electrons transfer from donor sites to acceptor sites. This is because the initial I_β phase is close to *the effective CT region* of β-spin electrons (vertically shadowed region in Fig. 8), where $|E_\beta(\eta_\alpha, \eta_\beta)|$ is as small as T. From the I_β phase, $(\eta_\alpha, \eta_\beta)$ approaches to the effective CT region by both α- and β-spin excitation (square and triangle marks in Fig. 8). Thus they work *constructively* for induction of phase conversion.

2. Temporal evolution from N phase

Next, we proceed to the dynamics of $(\eta_\alpha, \eta_\beta)$ starting from the N phase. The trajectories of $(\eta_\alpha, \eta_\beta)$ are shown in Fig. 10 under several different excitation conditions. When a small amount of β-spin electrons are excited, it results in a local oscillation [inset of Fig. 10, for $(\phi_\alpha, \phi_\beta) = (0,0.01)$], as expected. On the other hand, when a larger amount of β-spin electrons than the threshold value are excited, phase conversions between the N and I_β phases occurs [solid curve in Fig. 10, for $(\phi_\alpha, \phi_\beta) = (0,0.01)$]. These two types of dynamics can be clearly distinguished at the threshold value for ϕ_β.

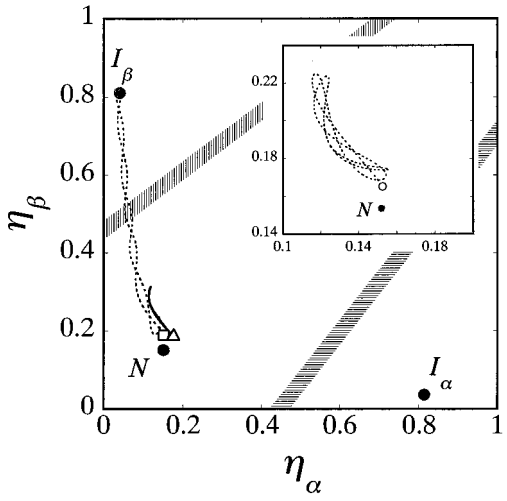

FIG. 10. Temporal trajectories of $(\eta_\alpha, \eta_\beta)$ after photoinjection into the N phase; solid [broken] curve for $(\eta_\alpha, \eta_\beta) = (0.02,0.06)$ [(0, 0.06)]. The square and triangle marks represent the initial condition just after photoexcitation. Inset: motion of $(\eta_\alpha, \eta_\beta)$ for $(\eta_\alpha, \eta_\beta) = (0,0.02)$.

As long as only β-spin electrons are excited, η_α is kept almost constant as described above, i.e., only CT of β-spin electrons takes place.

The condition on $(\phi_\alpha, \phi_\beta)$ for induction of phase conversions is shown in Fig. 11. As we increase ϕ_α, the threshold value for ϕ_β becomes larger, and finally clear distinction between the two types of dynamics is lost. Such behavior can be understood by the phenomenological bistable model in Sec. II, assuming that η_α is kept constant; the energy conversion between the two electronic states described by $a_\beta^\dagger$ and $d_\beta^\dagger$ occurs at $m_\beta = (U/M - 1)\eta_\alpha + (\Delta - U)/2M$ [see Eq. (30)], which becomes larger as η_α is increased, i.e., the energy difference between N and I phases increases and degeneracy between these two states is gradually lost.

The crucial difference between the dynamics after photoinjection into N and I_β phases is that α- and β-spin excitations work *destructively* for induction of phase conversion from the N phase (see Fig. 11), while they work construc-

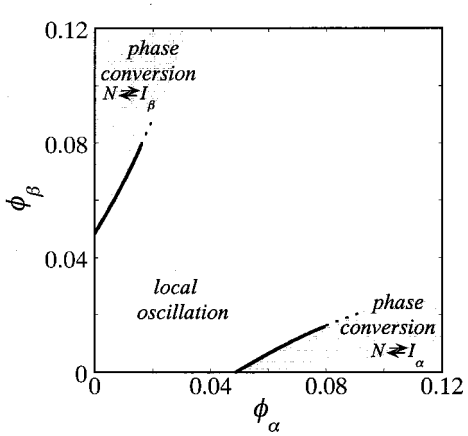

FIG. 11. Relation between the excited fraction $(\phi_\alpha, \phi_\beta)$ and its resultant dynamics, starting from the N phase. The dynamics changes discontinuously at the solid ''phase'' boundaries, while it changes continuously around the dotted ones.

tively from the I_β phase (see Fig. 9). The reason is simply understood with the help of Fig. 10. When only β-spin electrons are excited, $(\eta_\alpha, \eta_\beta)$ approaches to the effective CT region of β-spin electrons (square mark in Fig. 10), but when α-spin electrons are also excited simultaneously, the distance to the effective CT region becomes larger (triangle mark in Fig. 10). Thus we conclude that phase conversion from the N to I_β phase can be induced when $\phi_\beta - \phi_\alpha$ is large.

It should be noted that when equal amount of α- and β-spin electrons are excited, i.e., $\phi_\alpha = \phi_\beta$, the system is reduced to the bistable model with $m = (\Delta - U)/2(2M - U)$ by putting $\eta_\beta = \eta_\alpha$. In this direction on the $(\eta_\alpha, \eta_\beta)$ plane, there is no bistability under our choice of parameters (m never lies in the region of $0 < m < 1$), so the injected CT electron-hole pairs proliferates only very weakly.

D. Summary and remarks

By applying the UHF approximation to the modified Hubbard model, we have revealed that the energy conversion between one-electronic states actually occurs in this system, depending on η_α and η_β, the degrees of CT for α- and β-spin electrons. Under our choice of parameters, there are three stable states (N, I_α, and I_β phase), which are almost degenerate. Then we have demonstrated that phase conversion can be certainly induced by injection of small amount of excitations. The relation between the excited fraction $(\phi_\alpha, \phi_\beta)$ and its resultant dynamics is summarized in Fig. 9 (from the I_β phase) and Fig. 11 (from the N phase). ϕ_α and ϕ_β works constructively for induction of phase conversion from the I_β phase, while they work destructively from the N phase. This can be understood by the distance on the $(\eta_\alpha, \eta_\beta)$ plane between the initial positions just after photoexcitation (square and triangle marks in Figs. 8 and 10) and the effective CT region (shadowed region).

The dynamics discussed in this section is, even after the simplification (35), much more complicated than the dynamics of the phenomenological bistable model discussed in Sec. II. However, we can qualitatively understand the results obtained in this section with the help of the bistable model, owing to the fact that the effective CT region for α- and β-spin electrons are separated on the $(\eta_\alpha, \eta_\beta)$ plane; while CT of β- (α-) spin electrons is in progress, the CT degree for α- (β-)spin electrons remains almost constant, so the physical situation can be effectively described by the bistable model in Sec. II.

We mention here the deficiencies introduced through the UHF treatment of the electrons. Both the neutral and ionic phases are classified as insulators or semiconductors, but the physical origins of the insulating mechanisms are quite different. The neutral phase is characterized as a band insulator, where the UHF description of the ground state works well. On the other hand, the ionic phase is characterized as a Mott insulator, where the spin fluctuations play an important role and the low-energy properties are described by the antiferromagnetic (AF) Heisenberg Hamiltonian. In the UHF treatment employed in this study, due to the neglect of the spin fluctuations, the ionic phase is described by the I_σ phase, which is a Néel state with finite sublattice magnetization. Such a description is valid for higher-dimensional or anisotropic CT complexes. For an isotropic one-dimensional system, however, the ground state of the AF Heisenberg Hamiltonian is not appropriately described by the Néel state because spin fluctuations become more effective, and the sublattice magnetization disappears. Furthermore, in the presence of electron-lattice coupling, this state has an instability against dimerization through the spin-Peierls mechanism. One should take account of the spin fluctuations in order to overcome these deficiencies peculiar to the one-dimensional system. By the UHF approximation, we have also neglected the many-body effects such as the scattering among the careers due to Coulomb interaction, which is described by the four-operator terms.[13] This effect, together with the scattering by phonons and impurities, causes relaxation of the coherent dynamics, such as dephasing and energy dissipation.

It may look strange that we have employed two Néel states (I_α and I_β phases) as the ionic phase in our treatment, although the mathematically rigorous ground state of the AF Heisenberg Hamiltonian is, in any dimension, uniquely given by the singlet state. The singlet ground state is, however, accompanied by gapless spin-wave excitations, which originates from the Goldstone mode, i.e., simultaneous rotation of all spins. The substantial ground states should be interpreted as those states with broken rotational symmetry, which are degenerate due to the choice of the direction, as realized in the ferromagnetic Hamiltonian. In our consideration, we have broken the symmetry by fixing the axis, so the two Néel states with opposite directions are emphasized as a result.

The other approximation is the equivalent treatment of one-electronic states with the same spin, i.e., we have neglected the k dependence of the CT interaction T_k and that of the dipole coupling to photon field. The dipole coupling is proportional to $\sin k$ and is strong around $|k| \sim \pi/2$, contrary to the CT interaction T_k. We have confirmed that this approximation yields only small quantitative change to the dynamics, by comparing to the calculations without this approximation, i.e., the discrimination among one-electronic states by k is taken into account, with initial condition that the electrons with $|k| \sim \pi/2$ are excited simultaneously.

IV. CONCLUSIONS AND FURTHER PROBLEMS

In conclusion, we have shown the possibility of electronic phase conversions in multistable electronic systems, by exciting small fraction of ground-state electrons in one of the (meta)stable states. The essence of self-proliferation of the excited states is essentially included in the phenomenological bistable model; in those systems where energy conversion of one-electronic states is brought about by the whole electronic states in the system, transformation of electronic states occurs adiabatically in the neighborhood of the energy-conversion point, which promotes further transformation by itself. From the metastable phase, depending on whether the fraction ϕ of injected excitations is larger than the threshold value $\phi_{\mathrm{I-II}}$ or not, the excitation results in the following two qualitatively different dynamics: local oscillation around the initial state ($\phi < \phi_{\mathrm{I-II}}$) or macroscopic phase conversions ($\phi_{\mathrm{I-II}} < \phi$). From the stable phase, on the other hand, the dynamis changes continuously between those two patterns by changing ϕ. Thresholdlike behavior in ϕ can be observed

from both phases only when two phases are almost degenerate.

Next, we have demonstrated how the above mechanism is realized in the modified Hubbard model, which describes the electrons in mixed-stack CT complexes. Under our choice of the parameters, the system possesses three stable states (N, I_α, and I_β phases) which are almost degenerate. By applying the UHF approximation, we have shown that the energy conversion between one-electronic states described by $d^\dagger_{k\sigma}$ and $a^\dagger_{k\sigma}$ occurs two dimensionally, depending on the CT degrees η_α and η_β for α- and β-spin electrons. By exciting some amount of electrons [$\phi_{\alpha(\beta)}$ for $\alpha(\beta)$-spin electrons], phase conversions can be induced from each phase. From the I_β phase, α- and β-spin excitations work constructively for induction of phase conversion, while they does destructively from the N phase. This behavior can be understood by the geometrical relation on the $(\eta_\alpha, \eta_\beta)$ plane between the initial phases and the effective CT region, where the energy conversion between one-electronic states takes place.

In order to understand the photoinduced phase transition in the mixed-stack CT complexes, the following two effects should also be considered. (i) Although we have employed the infinite-range form of the intersite Coulomb interaction [the last term in Eq. (22)], it depends on the distance between the molecules in reality. Such a situation can be considered by the ΔUVT model, which is a complementary model to the ΔUMT model discussed in this paper. In the ΔUVT model, nearest-neighbor Coulomb interaction (V) is employed instead of Madelung energy (M), and stability of the electronic state of a DA pair is locally determined by the electronic states of neighboring DA pairs. When the N and I phases are degenerate, the number of the boundaries between N and I phases becomes a good quantum number to specify the excited states instead of the number of CT electron-hole pairs.[14] Then, the phase conversion can be induced by injection of only *a single CT exciton* but takes much longer time (proportional to the size of the system N) than is predicted in this study. (ii) The other effect neglected in this study is the electron-lattice coupling. The ionic phase has an instability against dimerization by the spin-Peierls mechanism, through which the magnetic properties of the ionic phase is qualitatively altered. The electron-phonon coupling will be reinvestigated to compare with our purely electronic treatment.

ACKNOWLEDGMENTS

The authors are grateful to Professor S. Koshihara and Professor K. Tanimura for detailed information on the experiments and to Professor K. Kitahara and Professor N. Nagaosa for discussions. One of the authors (K.K.) is grateful for discussions with Dr. H. Yokoyama, Dr. H. Kusunose, and other members of Professor Y. Kuramoto's group, and members of the condensed-matter theory group of ETL. This work was partly supported by a Grant-in-Aid for Scientific Research on Priority Areas, ''*Photoinduced Phase Transitions and Their Dynamics*,'' from the Ministry of Education, Science, Sports and Culture.

*Present address: Frontier Research System, The Institute of Physical and Chemical Research (RIKEN), Hirosawa 2-1, Wako, Saitama 351-0198, Japan; electronic address: koshino@cmpt.phys.tohoku.ac.jp

†Electronic address: ogawa@cmpt.phys.tohoku.ac.jp

[1] *Relaxations of Excited States and Photo-Induced Structural Phase Transitions*, edited by K. Nasu (Springer, Berlin, 1997).

[2] M. Le Cointe, M.H. Lemee-Cailleau, H. Cailleau, B. Toudic, L. Toupet, G. Heger, F. Moussa, P. Schweiss, K.H. Kraft, and N. Karl, Phys. Rev. B **51**, 3374 (1995).

[3] S. Koshihara, Y. Takahashi, H. Sakai, Y. Tokura, and T. Luty, J. Phys. Chem. B **103**, 2592 (1999).

[4] S. Koshihara, Y. Tokura, K. Takeda, and T. Koda, Phys. Rev. Lett. **68**, 1148 (1992).

[5] *Relaxation in Polymers*, edited by T. Kobayashi (World Scientific, Singapore, 1993).

[6] H. Okamoto, Y. Oka, T. Mitani, and M. Yamashita, Phys. Rev. B **55**, 6330 (1997).

[7] S. Koshihara, A. Oiwa, M. Hirasawa, S. Katsumoto, Y. Iye, C. Urano, H. Takagi, and H. Munekata, Phys. Rev. Lett. **78**, 4617 (1997).

[8] A.J. Heeger, S. Kilveson, J.R. Shrieffer, and W.-P. Su, Rev. Mod. Phys. **60**, 781 (1988).

[9] K. Iwano, J. Phys. Soc. Jpn. **66**, 1088 (1997).

[10] H.M. McConnell and R.J. Lynden-Bell, J. Chem. Phys. **36**, 2393 (1963).

[11] P.J. Strebel and Z.G. Soos, J. Chem. Phys. **53**, 4077 (1970).

[12] T. Iizuka-Sakano and Y. Toyozawa, J. Phys. Soc. Jpn. **65**, 671 (1996).

[13] H. Haug and S.W. Koch, *Quantum Theory of the Optical and Electronic Properties of Semiconductors* (World Scientific, Singapore, 1990).

[14] N. Nagaosa and J. Takimoto, J. Phys. Soc. Jpn. **55**, 2735 (1986); **55**, 2745 (1986).